

*Review Article (Invited)***Multistep growth of amyloid intermediates and its inhibition toward exploring therapeutic way: A case study using insulin B chain and fibrinogen**Naoki Yamamoto<sup>1</sup>, Eri Chatani<sup>2</sup><sup>1</sup> School of Medicine, Jichi Medical University, Shimotsuke, Tochigi 329-0498, Japan<sup>2</sup> Graduate School of Science, Kobe University, Kobe, Hyogo 657-8501, Japan

Received January 11, 2022; Accepted May 2, 2022;  
Released online in J-STAGE as advance publication May 10, 2022  
Edited by Yuji Goto

It is crucial to understand the mechanism of amyloid fibril formation for the development of the therapeutic ways against amyloidoses and neurodegenerative diseases. Prefibrillar intermediates, which emerge prior to the fibril formation, seem to play a key role to the occurrence of nuclei of amyloid fibrils. We have focused on an insulin-derived peptide, B chain, to precisely clarify the mechanism of the fibril formation via prefibrillar intermediates. Various kinds of methods such as circular dichroism spectroscopy, dynamic light scattering, small-angle X-ray scattering, and atomic force microscopy were employed to track the structural changes in prefibrillar intermediates. The prefibrillar intermediates possessing rod-shaped structures elongated as a function of time, which led to fibril formation. We have also found that a blood clotting protein, fibrinogen, inhibits the amyloid fibril formation of B chain. This was caused by the stabilization of prefibrillar intermediates and thus the suppression of their elongation by fibrinogen. These findings have not only shed light on detailed mechanisms about how prefibrillar intermediates convert to the amyloid fibril, but also demonstrated that inhibiting the structural development of prefibrillar intermediates is an effective strategy to develop therapeutic ways against amyloid-related diseases. This review article is an extended version of the Japanese article, *Observing Development of Amyloid Prefibrillar Intermediates and their Interaction with Chaperones for Inhibiting the Fibril Formation*, published in *SEIBUTSU BUTSURI* Vol. 61, p.236-239 (2021).

**Key words:** amyloid fibril, prefibrillar intermediate, nucleation mechanism, amyloid inhibitor, inhibition mechanism

**◀ Significance ▶**

Understanding molecular mechanisms about how prefibrillar intermediates, which accumulate prior to the amyloid fibril formation, convert to amyloid fibril is crucial for exploring therapeutic ways against amyloid-related diseases. We have developed a model system suitable for this purpose using an insulin-derived amyloid-prone peptide and fibrinogen as an amyloid inhibitor, in which it was shown that preventing the structural development of prefibrillar intermediate is crucial for the inhibition of fibril formation.

**Introduction**

Amyloid fibril is abnormal protein aggregates caused by protein misfolding, which is composed of stacked  $\beta$ -sheet structures accumulating on the fibril axis [1]. Deposition of amyloid fibrils in tissues or organs results in various diseases

Corresponding author: Naoki Yamamoto, School of Medicine, Jichi Medical University, 3311-1, Yakushiji, Shimotsuke, Tochigi 329-0498, Japan. ORCID iD: <https://orcid.org/0000-0003-0719-5157>, e-mail: [nyamamoto@jichi.ac.jp](mailto:nyamamoto@jichi.ac.jp)

referred to as amyloidoses [2]. For example, deposition of mutated transthyretin amyloids in peripheral nerves, heart, kidney, intestine, or eyes causes these tissues' dysfunction (familial amyloidosis). Overexpression of the light chain of monoclonal  $\gamma$ -globulin by abnormal marrow plasma cells results in the formation of amyloid fibrils and their deposition in various organs (systemic amyloidosis). Amyloid fibrils are also related to various diseases in the central nerve system known as neurodegenerative diseases [2]. For example, deposition of amyloid fibrils made of A $\beta$  peptide in the senile plaques is related to the onset of Alzheimer's disease. Parkinson's disease accompanies the accumulation of amyloid fibrils made of  $\alpha$ -synuclein in the Lewy body in neurons. Therefore, understanding the mechanism of amyloid fibril formation is crucial for designing strategy to prevent and cure these amyloidoses and neurodegenerative diseases.

Detailed structural information of the amyloid fibrils is now available due to the recent gigantic progress in the cryogenic electron microscopy (cryo-EM) [3,4]. The structural details in the atomic resolution are useful to understand how amyloid fibrils are stabilized, and also the reason why various fibril forms are generated from one amino-acid sequence (polymorphism). However, in the viewpoint of combatting the amyloid-related diseases, it would be too late to treat after amyloid fibrils appear, because the symptoms would already be progressing. Therefore, preventing the formation of amyloid fibrils prior to their maturation and accumulation must be requisite for the treatment of the diseases.

As shown in Figure 1, it has been proposed that the onset of amyloid formation requires the formation of a nucleus which works as a template of the fibril elongation [4]. Copying the structure of the nucleus continuously occurs upon the association of monomers with the nucleus, leading to the elongation of the fibril structure. Understanding how the nucleus is formed is a key to clarification of the mechanism of amyloid fibril formation. Two different mechanisms of the nucleus formation are so far proposed (Figure 2) [5,6]. One is the nucleation-growth (NG) model (Figure 2, top). In this model, monomeric polypeptide chains interact with each other with searching a fibril conformation. However, fibril structure cannot be stabilized due to inadequate interactions unless it grows to a certain size. In the middle way of the size growth, there is a state where the free energy becomes highest. This highest energy state is defined as a nucleus, which is difficult to be observed. The nucleus can be both monomeric or aggregates of monomers. Further association of monomers results in lowering the free energy. On the other hand, in the nucleus conformational conversion (NCC) model, stable oligomers, or prefibrillar intermediates, are first formed, followed with a conversion to nuclei (Figure 2, bottom). Similar to the case of NG model, decrease in the free energy is achieved by structural changes around nuclei. In this case, the nucleation would not require as much activation energy as that in the NG model, because the prefibrillar intermediates could work to stabilize the nucleus. Although these NG and NCC models are distinguished from each other as different mechanisms, both of them would exist in parallel in a realistic case.

However, the NCC model would be dominant in a situation where the concentration of amyloid-prone proteins or peptides is high, because the formation of oligomeric prefibrillar intermediates is caused by intermolecular interactions. For example, it is known that patients with Down syndrome, which originates from trisomy 21 (3 copies of the chromosome 21 instead of 2 copies), possess much higher risk to contract Alzheimer's disease [7]. In this case, the causative gene for the protein related to Alzheimer's disease (amyloid precursor protein) also exists in chromosome 21 and thus results in producing higher concentration of A $\beta$  peptide than usual [8]. In this regard, preventing the formation of the prefibrillar intermediates or their conversion to amyloid fibrils is a reasonable strategy to cure amyloid-related diseases.

Moreover, physiological conditions such as pH and salt concentration are also important factors to determine which pathway is dominant. If the value of pH is close to an isoelectric point of a protein, it becomes easy to form oligomers because of weak electric repulsion among

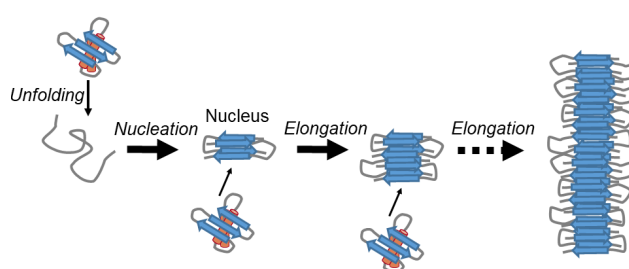


**Figure 1** A schematic picture of the amyloid fibril formation. The nucleus which is formed by the unfolded proteins plays a role as a template for the fibril elongation by recruiting monomeric proteins.

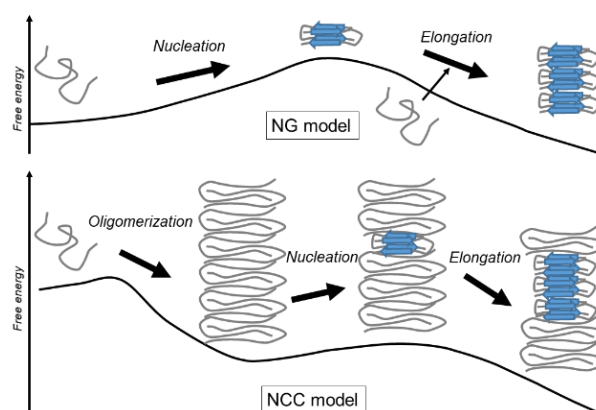


**Figure 2** Schematic descriptions of NG and NCC models. In each model, free energy level is shown by a line.  $\beta$ -sheet structures are written by blue. See detail in the text.

monomers. Moreover, high salt concentration also reduces the electric repulsion, resulting in favoring the NCC model. Actually, it was reported that formation of prefibrillar intermediates were induced in a high salt-concentration condition [9]. Therefore, which model, NG or NGG, is favored would depend on these factors in the realistic case.

Though a large number of researches have been performed to understand how prefibrillar intermediates convert to amyloid fibrils, an underlying molecular mechanism is not fully understood yet [10-13]. According to literature, two factors seem to be requisite for propelling researches related to prefibrillar intermediates; ease to obtain an amyloid-prone protein, and efficient accumulation of its prefibrillar intermediates. Further, it would be desirable if any amyloid inhibitors against the protein is found, so that we can also learn how to prevent the amyloid fibril formation by targeting prefibrillar intermediates.

### Established Model System; Insulin B chain and Fibrinogen

With this background, we have found a model case of prefibrillar intermediates converting to the amyloid fibrils in an insulin-derived peptide, insulin B chain. Insulin is composed of A chain and B chain, which are covalently connected by two disulfide bonds (Figure 3A) [14]. B chain can be easily obtained by cleaving the disulfide bonds using reducing reagents such as dithiothreitol (Figure 3B). Insulin amyloid fibrils are responsible for the occurrence of an “insulin ball”, which accumulates in a subcutaneous tissue where insulin is continuously injected for the treatment of diabetes [15]. Some researches mentioned the possibility that B chain also participates in this syndrome [16,17]. B chain is composed of 30 amino acids, and the isoelectric point of the polypeptide is around 7.8. Another advantage of the system is that large amount of prefibrillar intermediates accumulates prior to the amyloid fibril formation [18]. Furthermore, we have found that the fibril formation is inhibited by a blood clotting protein, fibrinogen (Fg) [19]. These features are suitable for the investigation of the mechanisms of the formation and inhibition of amyloid fibrils occurring via prefibrillar intermediates. In this review article, we overview the structural properties of the prefibrillar intermediates and their complex with Fg, and give perspective how these systems is applicable for the treatments of the amyloid-related diseases.

### Accumulation of Prefibrillar Intermediates in Insulin B chain

B chain possesses a monomeric random-coil structure in 10 mM NaOH solution. However, if the value of pH gets closer to its isoelectric point (pH ~7.8), aggregation easily occurs due to the reduction of the electrostatic repulsion. Using this property, the fibril formation reaction was initiated by the pH jump from ~11 to 8.7 (Figure 3C) [18]. To accelerate amyloid fibril formation, the sample was shaken at 1,200 rpm, which we call an agitated condition (Figure 4A). In this condition, fibril formation, monitored by thioflavin T (ThT) fluorescence, completed within two hours (Figure 4A, black points). The formation curve seems to be a typical sigmoidal curve observed in a standard amyloid fibril formation. Atomic force microscopy (AFM) showed the formation of amyloid fibrils (Figure 4B, left). However, a slight increase in ThT intensity was observed in the early stage, indicative of the accumulation of prefibrillar intermediates (Figure 4A, inset). The structural development in this early time stage was investigated in a quiescent condition, in which no agitation was applied to the sample (Figure 4A, red points). As expected, the period of accumulation of prefibrillar intermediates prolonged at least up to a day. Furthermore, a large number of particles were observed by AFM (Figure 4B, right). The circular dichroism (CD) spectra of the prefibrillar intermediates shifted to the direction where secondary structure were formed (Figure 4C). In the time course, a bi-exponential behavior was observed where the first quick change occurred with a time constant of ~20 min, followed by a slow change whose time constant was ~500 min (Figure 4E). A time course of the molecular size was also monitored by dynamic light scattering (DLS) (Figure 4D). The hydrodynamic diameter,  $D_h$ , increased as a function of time. Furthermore, the hydrodynamic diameter increased in a bi-exponential

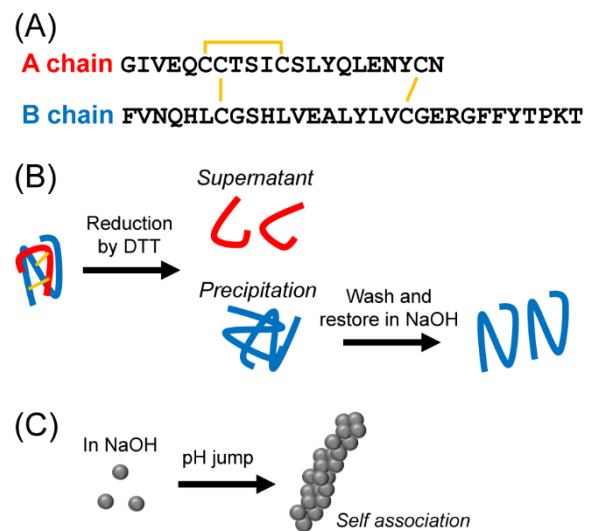


**Figure 3** Property of insulin B chain. (A) The amino acid sequences of insulin A chain and B chain. The disulfide bonds are shown by the yellow lines. Two of the three disulfide bonds connect the two chains. (B) The purification process of B chain (blue) from A chain (red). Reduction of the disulfide bonds (yellow) by dithiothreitol (DTT) causes B chain precipitation while A chain remaining in solution at pH 8.7. The precipitated B chain is washed by water and dissolved in 10 mM NaOH. (C) Monomeric B chain in NaOH solution self-associates upon jumping pH values to lower one such as 8.7.

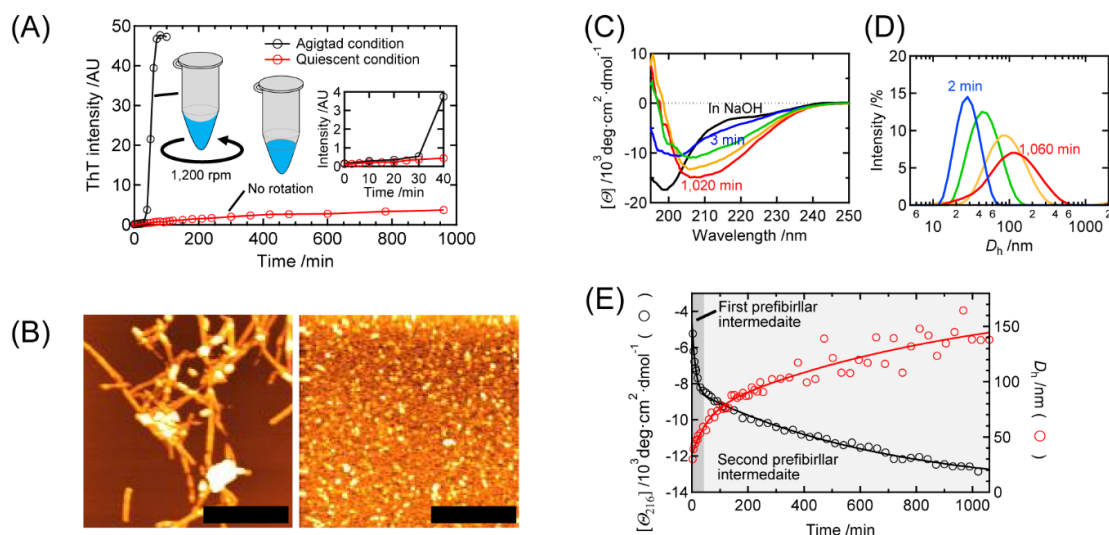


**Figure 4** Amyloid fibril formation and accumulation of the prefibrillar intermediates of B chain in the agitated and quiescent conditions, respectively, at the concentration of 1.4 mg/ml. (A) Time-dependence of ThT fluorescent intensity in the agitated and quiescent conditions. In the agitated condition where the sample tube is rotated at 1,200 rpm, the amyloid fibril formation is stimulated. On the contrary, in the quiescent condition where no rotation is applied to the sample tube, prefibrillar intermediates accumulate. Schematic pictures describing these two situations are drawn along with the data. The inset shows the plots in the early time stage. Prior to the fibril formation, a slight increase due to formation of prefibrillar intermediate is observed in the early time stage. (B) AFM images of amyloid fibrils observed in the agitated condition (left) and particles confirmed at 60 min in the quiescent condition (right), respectively. The scale bars indicate 2  $\mu\text{m}$ . (C) Time-course of CD spectra in the quiescent condition. The spectrum in 10 mM NaOH is also shown. (D) Time-course of the hydrodynamic diameter in the quiescent condition obtained by DLS. (E) Time-dependences of the theta value at 216 nm in the CD spectra and the hydrodynamic diameter obtained from DLS. The solid lines represent fitting curves obtained by regression analyses. The graphs were constructed based on the results reported in [18].

manner with similar time constants to those obtained by CD. The hydrodynamic diameters of the first and second species were  $\sim 60$  and  $\sim 130$  nm, respectively (Figure 4E). We thus defined these two species as the first and second prefibrillar intermediates (Figure 4E). Solution-state NMR measurements revealed that  $\sim 60\%$  of B chain participated in the formation of the prefibrillar intermediates in this condition, which represents that this system is suitable to investigate the characteristics of the prefibrillar intermediates [18].

### Prefibrillar Intermediates Responsible for the Amyloid Fibril Formation

Declaring which prefibrillar intermediates are related to the amyloid fibril formation is crucial to understand the pathway of amyloid fibril formation. In literature, there are several novel methods to scrutinize the pathway where prefibrillar intermediates undergo the transformation to amyloid fibrils, such as solid-state nuclear magnetic resonance [20] or electron spin resonance [21], however, these methods require delicate sample preparations and analyses. Instead, we developed a way to use ultrasonic wave with referring to a literature where a continuous irradiation of ultrasonic wave accelerated an amyloid fibril formation [22]. A one-second ultrasonic wave pulse was applied at several time points (0 min, 30 min, 120 min, 253 min, and 420 min) in the middle way of the structural development of the prefibrillar intermediates, and structural change was traced by CD spectra (Figure 5). Immediately after the reaction started (0 min), no prefibrillar intermediate existed in the system. At 30 min, the formation reaction of the first prefibrillar intermediate was significantly progressed whereas almost no second prefibrillar intermediate existed. At 120 min and thereafter, the amount of the second prefibrillar intermediate was approximately proportional to the increase in time.

As a result, the amyloid fibril formation was induced when the second prefibrillar intermediate existed (Figure 5A). Furthermore, the speed of the formation was proportional to the amount of the second prefibrillar intermediates (Figure 5B). On the other hand, no fibril formation was confirmed when the first prefibrillar intermediate only existed, i.e. until 30 min of the reaction (Figure 5B). These results clearly demonstrated that the second prefibrillar intermediate and not the first one is responsible for the amyloid fibril formation (Figure 5C). Whereas, the first prefibrillar intermediate was assumed to be a mandatory one necessary for the formation of the second prefibrillar intermediate based on the fact that the size development was smooth between these two species (Figure 4E and 5C).



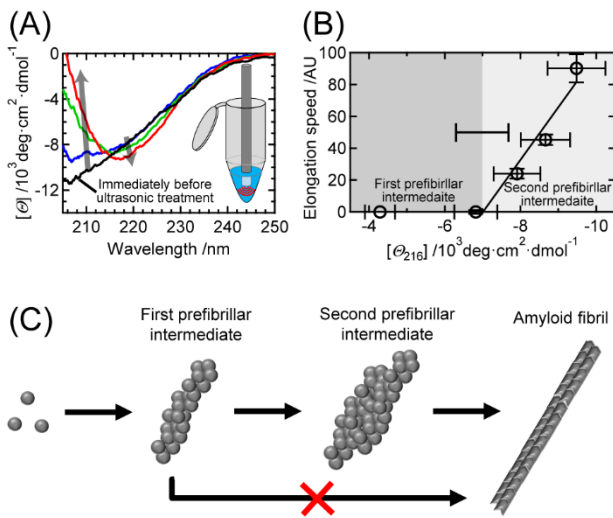


**Figure 5** Induction of the amyloid fibril formation from prefibrillar intermediates upon applying an ultrasonic wave pulse (1 sec) at 1.4 mg/ml B chain in the quiescent condition. (A) An example of the ultrasonic treatment applied at 120 min in the time course of the structural development of prefibrillar intermediates monitored by CD spectra. The time-dependent change is indicated by arrows. A schematic picture of the ultrasonic treatment on the sample is shown in the figure. (B) The relationship between the amount of the first or the second prefibrillar intermediate and the elongation speed of amyloid fibrils after the ultrasonic wave pulse is applied. The horizontal axis, which is the theta values proportional to the amount of the first or the second prefibrillar intermediate, increases as it goes to the right. (C) A schematic drawing of the fibril formation pathway proposed by the ultrasonic treatment experiment. The graphs were constructed based on the results reported in [18].

### Finding Amyloid Inhibitor Among Natural Proteins

Based on the finding above, suppressing the structural development of the prefibrillar intermediates could be a plausible strategy to inhibit the amyloid fibril formation. Molecular agents which specifically bind to monomers to inhibit formation of the prefibrillar intermediates is one possible way to execute it, though it might take so much time to find such specific molecules. Another strategy is targeting the prefibrillar intermediates themselves. This would rather be easier to execute by using a large molecule which can interact with the prefibrillar intermediates by taking advantage of their large surface. Natural proteins could be appropriate candidates in the latter case because of their large molecular size. Actually, there have been lots of intracellular molecular chaperones known to work to prevent protein misfolding and aggregation [23,24]. Furthermore, extracellular proteins such as clusterin,  $\alpha_2$ -macroglobulin, and haptoglobin can also possess chaperone-like activities [25]. Among them, we focused on a recent result reporting that Fg suppressed protein thermal aggregation and also inhibited an amyloid fibril formation [26,27].

Fg is a blood coagulation factor I participating in blood coagulation reaction, and the third most populated protein in plasma next to albumin and  $\gamma$ -globulin [28]. Its molecular weight is ~340 kDa, and the shape is a rod-like structure (Figure 6A) [29]. We have found that Fg can inhibit the amyloid fibril formation of B chain [19]. As shown in Figure 6B, Fg obviously inhibited the amyloid fibril formation in a concentration-dependent manner. The inhibition degree, evaluated by the ThT intensity after reaching equilibrium, was clearly Fg-concentration dependent (Figure 6C). To scrutinize the relationship between the inhibition and the extent of the interaction of Fg with prefibrillar intermediates, the concentration of Fg-bound prefibrillar intermediates at each Fg concentration was calculated using solution NMR. Fg signals completely overlapped with those of monomeric B chain, whereas signals in a histidine residue of B chain monomer was separable (Figure 6E). Thus, in the experiment, we focused on the signals originated from monomeric B chain. We took advantage of a property of the prefibrillar intermediates to dissociate to monomers upon dilution (Figure 6D, left). On the contrary, in the Fg-bound state, the prefibrillar intermediates become resistant to the dissociation (Figure 6D, right). In solution NMR, the dissociated or intrinsically-existing monomers can only be observed. In addition to this, it was confirmed that Fg did not bind to the monomer. Therefore, by monitoring signal intensities after the dilution, the concentration of Fg-bound prefibrillar intermediates can be estimated. The NMR spectra after dilution at various Fg concentrations are shown in Figure 6E. A peak originated from a histidine  $\epsilon$  proton (indicated by the arrow in Figure 6E) did not overlap with Fg signals, and thus was used for the analysis. The signal intensity decreased as a function of Fg concentration, representing that Fg apparently binds to the prefibrillar intermediates (Figure 6C). Furthermore, the decrease in intensity correlated with the degree of fibril formation inhibition (Figure 6C). This clearly represented that the binding of Fg with the prefibrillar intermediates is crucial for the inhibition. The dissociation constant was estimated by analyzing the concentration dependence, resulting in a sub- $\mu\text{M}$  value (Figure 6C), indicating that the interaction is strong. In addition to this, CD spectra, DLS and size exclusion chromatography (SEC) also supported this direct interaction of Fg with the prefibrillar intermediates [19]. In the estimation of the affinity coefficient, we assumed that both of the first and second prefibrillar intermediates participated in the formation of the complex with Fg at a same magnitude of affinity [19].

To obtain insight into molecular shapes of prefibrillar intermediates and their complex with Fg, small-angle X-ray scattering (SAXS) was performed. By analyzing the SAXS intensity as a function of the absolute value of the scattering

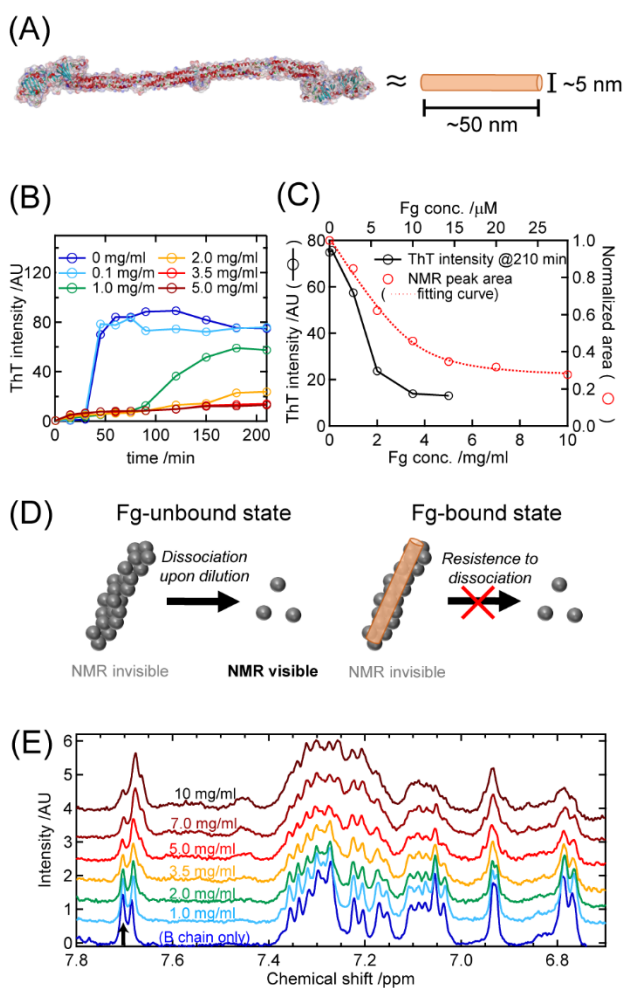


**Figure 6** Inhibition of the amyloid fibril formation by Fg at 1.4 mg/ml B chain. (A) The X-ray crystal structure of Fg described by the VDW surface. The ribbon model of the secondary structures is also overlaid with the surface mode. The size of an approximated rod-like structure is also shown. (B) Fg concentration dependency of the amyloid fibril formation in the agitated condition monitored by ThT fluorescence. (C) Fg concentration dependence of the ThT intensity at 210 min in panel A. A NMR peak area of B chain analyzed in panel E is also plotted. The value indicates the amount of Fg-unbound prefibrillar intermediates or monomers which intrinsically existed in the system. See detail in the text. The dash line represents a fitting curve obtained by a regression analysis using a model function to obtain the dissociation constant. (D) Schematic drawing of how to detect the monomeric B chain by solution NMR. In the Fg-unbound state, the prefibrillar intermediates easily dissociate into monomers upon dilution. On the other hand, the dissociation is hard to occur in the Fg-bound state (Fg is shown by the orange rod). In both cases, monomers and not prefibrillar intermediates are only visible by solution NMR. Using this property, the concentration of Fg-bound prefibrillar intermediates can be obtained. The detailed description is written in the text. (E) NMR spectra of B chain in the presence of Fg at various concentrations. B chain and Fg were incubated for 2 hours in the quiescent condition, diluted by 4-fold, and the NMR spectra were obtained. The arrow indicates the signal of a histidine  $\epsilon$  proton, which could be separated from Fg signals by a spectral deconvolution and thus was used for the analysis. The graphs were constructed based on the results reported in [18].

vector,  $q$ , molecular shapes can be estimated. The analysis was performed with the following equation;

$$\log I(q) = \log I(0) + a \cdot \log(q) \quad (1)$$

where  $I(q)$  and  $a$  represent the scattering intensity at  $q$  and the slope of the log-log plot, respectively. It is known that the slope of a rod-like structure is  $\sim -1$  [30]. As shown in Figure 7A, the slope of Fg was  $\sim -1$ , consistent with the fact that the structure is approximately rod-shaped (Figure 6A). Interestingly, the slopes of the prefibrillar intermediates and also their complex with Fg were also close to  $-1$  (Figure 7A), representing that they also possess rod-like structures. In this case, the base diameter of a rod,  $D_p$ , can be calculated using the cross-section plot. The plot is generated by multiplying  $q$  to the both axes of the log-log plot so that the dimension of the length disappears.  $D_p$  can be evaluated fitting the following equation to the plot (Figure 7B);

$$\log\{I(q) \cdot q\} = A - \frac{D_p^2}{16} q^2 \quad (2)$$

where  $A$  represents an intercept. The obtained  $D_p$  of Fg was  $\sim 5$  nm, which was consistent with its crystal structure (Figure 6A).  $D_p$  of the prefibrillar intermediates was  $\sim 7$  nm in average, and the value increased to  $\sim 14$  nm upon the formation of the complex with Fg (Figure 7B and C). Based on these results, we proposed that seven Fg molecules surround the circumference of rod-like prefibrillar intermediates in parallel to their axes, which comprises one complex unit (Figure 7C). The molecular ratio of B chain:Fg calculated from this model was consistent with that obtained by the NMR analysis (B chain:Fg  $\sim 30:1$ ), and thus validity of the model was confirmed [19]. Taken these results together, it was concluded that the interaction of Fg plays a role to stabilize the prefibrillar intermediates and also to suppress the amyloid fibril formation.

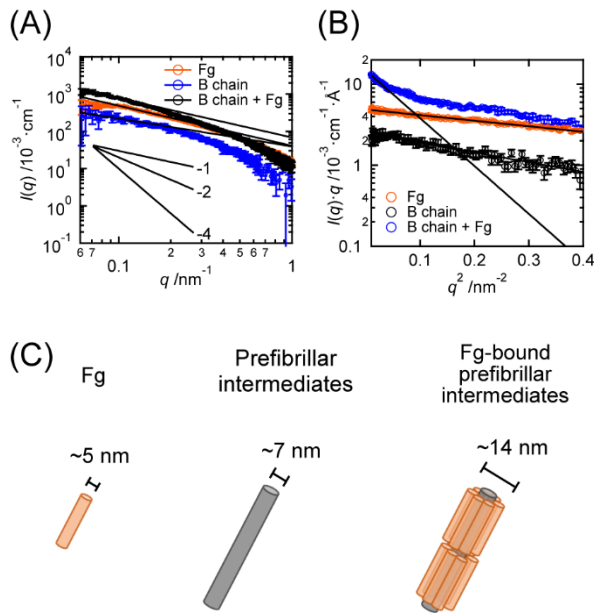


**Figure 7** SAXS analyses and the resultant molecular models of prefibrillar intermediates and their complex with Fg. (A) The log-log plot of the scattering intensity as a function of  $q$ . The slopes represent the fitting curves obtained by the regression analysis using eq (1). The fitting region should satisfy with the condition,  $1/L < q < 1/D_p \text{ nm}^{-1}$  ( $L$  represents the length of the rod-like structure, which was also estimated from the SAXS analysis in literature (ref [19])). Examples of integer slopes are also shown in inset. (B) The cross-section plot for the analysis of the base diameter. The lines represent the fitting curves obtained by the regression analysis using eq (2). The fitting region should satisfy with the condition,  $D_p \cdot q < 3.7$ . (C) Molecular shapes of a prefibrillar intermediate and its complex with Fg obtained by the SAXS analyses. Each species possesses a rod-shaped structure. The base diameter obtained from the cross-section plot is shown on each species.

Attempt was paid to acquire images of the prefibrillar intermediates and the complex with Fg using AFM to support the result of SAXS. However, small particles, and not rod-like structures as expected by the SAXS analysis, had only been observed (Figure 4B, bottom) [18,19]. It seemed that this is due to the nature of prefibrillar intermediates easily dissociating into monomers upon dilution, which would occur during washing mica substrates in the AFM sample preparation process. We thus performed TEM measurement in which samples adsorbed on a thin carbon film is fixed by using dyes such as uranyl acetate. As a result, prefibrillar intermediates, possessing long wavy structures were clearly observed [31]. Furthermore, suppression of the elongation of prefibrillar intermediates and inhibition of the amyloid fibril formation by Fg was also clearly confirmed by TEM [31].

### Proposed Scheme and Its Generality in the Amyloid Study

The overall picture of the structural development of B chain prefibrillar intermediates and its inhibition by Fg is shown in Figure 8. At least two kinds of intermediates, i.e. the first and second prefibrillar intermediates exist, which possess rod-like structures. The second prefibrillar intermediate, which is longer than the first one, is the species responsible for the amyloid fibril formation. As indicated in the latest study, a nucleus forms from in the second prefibrillar intermediate. The prefibrillar structure could propagate so that amyloid fibrils are formed [31]. Fg binds on the circumference of the prefibrillar intermediates, and suppresses the amyloid fibril formation. Structural stabilization of the prefibrillar intermediates by Fg inhibits further elongation of the prefibrillar intermediate, which could be responsible for the inhibition of amyloid fibril formation. In addition to this, Fg may also contribute to hindrance of monomer attachments to prefibrillar intermediates.

As mentioned above, we demonstrated that the filamentous intermediates of insulin B chain are responsible for the amyloid fibril formation. Then, how general it would be? Actually, there have been several reports showing that the elongation of such structures plays a key role for amyloid fibril formation. For example, an insulin helical hexamer formed in a beads-on-string manner constructs protofilaments that could finally change to amyloid fibrils [32]. It was suggested that this hexamer was a building block for the amyloid fibril formation. In a case of glucagon, the diameter and length of the intermediates developed as a function of time, which finally led to the formation of matured amyloid fibrils [33]. It was concluded that the intermediates are on-pathway species that easily convert to mature amyloid fibrils. Taken together, formation of these rod-shaped prefibrillar intermediates would work as a reaction field where the nucleation and following propagation efficiently occurs.

### Conclusions and Perspectives

As we reviewed here, prefibrillar intermediates easily occur when protein concentration is high enough to promote intermolecular interactions under appropriate reaction conditions. Thus, prefibrillar intermediates would play a main role to facilitate amyloid fibril formation if the protein concentration is intrinsically high (e.g. light chain of  $\gamma$ -globulin produced by abnormal marrow plasma cells), or its localization occurs for some reasons (e.g. insulin in insulin balls). In this situation, suppressing interconversion from prefibrillar intermediates to amyloid fibrils is requisite to prevent

amyloid-related diseases. Using Fg, we have here shown that it is not so difficult to achieve the mission. Interestingly, the physiological concentration of Fg in blood (2-6 mg/ml) is in the same order as that used to efficiently suppress the B chain amyloid fibril formation in our study. Therefore, inhibition of the fibril formation by such extracellular proteins would actually be occurring constantly in our body, which might work as an “innate immune system” to prevent amyloid-related diseases. Recent finding, another non-chaperone extracellular proteins inhibiting amyloid fibril formation, also strengthens this idea [34].

In addition to danger which is brought by amyloid fibril formation, cell toxicity of prefibrillar intermediates is also another concern. For example, it has been said that A $\beta$  oligomers, which emerge prior to the amyloid fibril formation are more cytotoxic than amyloid fibrils [5]. Therefore, suppressing its toxicity has to be taken into consideration for the therapeutic ways. We have preliminary found that Fg not only inhibits the amyloid fibril formation of A $\beta$ , but also suppresses the cytotoxicity of A $\beta$  oligomers which accumulate prior to the fibril formation (manuscript to be submitted). This result shows that amyloid inhibitors could also be used as efficient reducers of cytotoxicity of prefibrillar intermediates. In this viewpoint, naturally-occurring chaperone-like proteins such as Fg are good candidates for the therapeutic methods in the sense that few side effects are expected to be caused. Exploring new potential usages of the molecular chaperones will accelerate the development of efficient therapeutic agents against amyloid-related diseases.

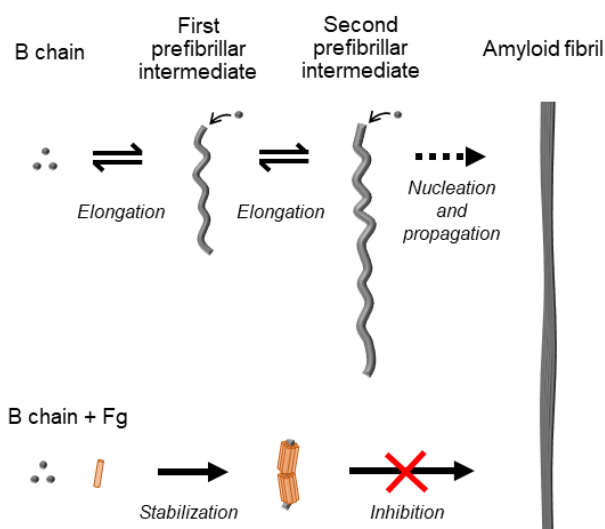


**Figure 8** Molecular mechanism of the structural development of the prefibrillar intermediates (top), and the inhibition by Fg (bottom). The drawing was prepared based on the result reported in ref [19] with modification.

### Conflict of Interest

There is no conflict of interest related to this review article.

### Author Contributions

N.Y. and E.C. wrote the manuscript.

### Acknowledgements

We would like to thank to the collaborators who participated in the studies related to this review: Prof. Rintaro Inoue and Masaaki Sugiyama (Kyoto University, Japan), Dr. Teruki Makino and Prof. Akira Naito (Yokohama National University, Japan), Prof. Naoya Shibayama (Jichi Medical University, Japan), and Mr. Taiki Akai, Ms. Shoko Tshuhara, and Prof. Atsuo Tamura (Kobe University, Japan). The graphical abstract was created by a designer, Y.Yamamoto.

### References

- [1] Dobson, C. M. Protein folding and misfolding. *Nature* 426, 884-890 (2003). <https://doi.org/10.1038/nature02261>
- [2] Landreh, M., Sawaya, M. R., Hipp, M. S., Eisenberg, D. S., Wuthrich, K., Hartl, F. U. The formation, function and regulation of amyloids: Insights from structural biology. *J. Intern. Med.* 280, 164-176 (2016). <https://doi.org/10.1111/joim.12500>
- [3] Chatani, E., Yuzu, K., Ohhashi, Y., Goto, Y. Current understanding of the structure, stability and dynamic properties of amyloid fibrils. *Int. J. Mol. Sci.* 22, 4349 (2021). <https://doi.org/10.3390/ijms22094349>
- [4] Iadanza, M. G., Jackson, M. P., Hewitt, E. W., Ranson, N. A., Radford, S. E. A new era for understanding amyloid structures and disease. *Nat. Rev. Mol. Cell Biol.* 19, 755-773 (2018). <https://doi.org/10.1038/s41580-018-0060-8>
- [5] Bemporad, F., Chiti, F. Protein misfolded oligomers: Experimental approaches, mechanism of formation, and structure-toxicity relationships. *Chem. Biol.* 19, 315-327 (2012). <https://doi.org/10.1016/j.chembiol.2012.02.003>
- [6] Chatani, E., Yamamoto, N. Recent progress on understanding the mechanisms of amyloid nucleation. *Biophys. Rev.* 10, 527-534 (2018). <https://doi.org/10.1007/s12551-017-0353-8>



- [7] Masters, C. L., Simms, G., Weinman, N. A., Multhaup, G., Mcdonald, B. L., Beyreuther, K. Amyloid plaque core protein in alzheimer-disease and down syndrome. *Proc. Natl. Acad. Sci. U.S.A.* 82, 4245-4249 (1985). <https://doi.org/10.1073/pnas.82.12.4245>
- [8] Shi, Y., Kirwan, P., Smith, J., MacLean, G., Orkin, S. H., Livesey, F. J. A human stem cell model of early alzheimer's disease pathology in down syndrome. *Sci. Transl. Med.* 4, 124ra29 (2012). <https://doi.org/10.1126/scitranslmed.3003771>
- [9] Chatani, E., Imamura, H., Yamamoto, N., Kato, M. Stepwise organization of the  $\beta$ - structure identifies key regions essential for the propagation and cytotoxicity of insulin amyloid fibrils. *J. Biol. Chem.* 289, 10399-10410 (2014). <https://doi.org/10.1074/jbc.M113.520874>
- [10] Lee, J., Culyba, E. K., Powers, E. T., Kelly, J. W. Amyloid- $\beta$  forms fibrils by nucleated conformational conversion of oligomers. *Nat. Chem. Biol.* 7, 602-609 (2011). <https://doi.org/10.1038/nchembio.624>
- [11] Bleiholder, C., Dupuis, N. F., Wyttenbach, T., Bowers, M. T. Ion mobility-mass spectrometry reveals a conformational conversion from random assembly to  $\beta$ -sheet in amyloid fibril formation. *Nat. Chem.* 3, 172-177 (2011). <https://doi.org/10.1038/Nchem.945>
- [12] Chimon, S., Shaibat, M. A., Jones, C. R., Calero, D. C., Aizezi, B., Ishii, Y. Evidence of fibril-like  $\beta$ -sheet structures in a neurotoxic amyloid intermediate of alzheimer's  $\beta$ -amyloid. *Nat. Struct. Mol. Biol.* 14, 1157-1164 (2007). <https://doi.org/10.1038/nsmb1345>
- [13] Nilsson, M. R., Dobson, C. M. Chemical modification of insulin in amyloid fibrils. *Protein Sci.* 12, 2637-2641 (2003). <https://doi.org/10.1110/ps.0360403>
- [14] Weiss, M. A. The structure and function of insulin: Decoding the tr transition. *Vitam. Horm.* 80, 33-49 (2009). [https://doi.org/10.1016/S0083-6729\(08\)00602-X](https://doi.org/10.1016/S0083-6729(08)00602-X)
- [15] Dische, F. E., Wernstedt, C., Westermarck, G. T., Westermarck, P., Pepys, M. B., Rennie, J. A., et al. Insulin as an amyloid-fibril protein at sites of repeated insulin injections in a diabetic patient. *Diabetologia* 31, 158-161 (1988). <https://doi.org/10.1007/Bf00276849>
- [16] Mori, W., Yuzu, K., Lobsiger, N., Nishioka, H., Sato, H., Nagase, T., et al. Degradation of insulin amyloid by antibiotic minocycline and formation of toxic intermediates. *Sci. Rep.* 11, 6857 (2021). <https://doi.org/10.1038/s41598-021-86001-y>
- [17] Yuzu, K., Lindgren, M., Nystrom, S., Zhang, J., Mori, W., Kunitomi, R., et al. Insulin amyloid polymorphs: Implications for iatrogenic cytotoxicity. *RSC Adv.* 10, 37721-37727 (2020). <https://doi.org/10.1039/d0ra07742a>
- [18] Yamamoto, N., Tshihara, S., Tamura, A., Chatani, E. A specific form of prefibrillar aggregates that functions as a precursor of amyloid nucleation. *Sci. Rep.* 8, 62 (2018). <https://doi.org/10.1038/s41598-017-18390-y>
- [19] Yamamoto, N., Akai, T., Inoue, R., Sugiyama, M., Tamura, A., Chatani, E. Structural insights into the inhibition of amyloid fibril formation by fibrinogen via interaction with prefibrillar intermediates. *Biochemistry* 58, 2769-2781 (2019). <https://doi.org/10.1021/acs.biochem.9b00439>
- [20] Chimon, S., Shaibat, M. A., Jones, C. R., Calero, D. C., Aizezi, B., Ishii, Y. Evidence of fibril-like  $\beta$ -sheet structures in a neurotoxic amyloid intermediate of alzheimer's  $\beta$ -amyloid. *Nat. Struct. Mol. Biol.* 14, 1157-1164 (2007). <https://doi.org/10.1038/nsmb1345>
- [21] Pavlova, A., Cheng, C. Y., Kinnebrew, M., Lew, J., Dahlquist, F. W., Han, S. Protein structural and surface water rearrangement constitute major events in the earliest aggregation stages of tau. *Proc. Natl. Acad. Sci. U.S.A.* 113, E127-E136 (2016). <https://doi.org/10.1073/pnas.1504415113>
- [22] Ohhashi, Y., Kihara, M., Naiki, H., Goto, Y. Ultrasonication-induced amyloid fibril formation of  $\beta_2$ -microglobulin. *J. Biol. Chem.* 280, 32843-32848 (2005). <https://doi.org/10.1074/jbc.M506501200>
- [23] Kim, Y. E., Hipp, M. S., Bracher, A., Hayer-Hartl, M., Hartl, F. U. Molecular chaperone functions in protein folding and proteostasis. *Annu. Rev. Biochem.* 82, 323-355 (2013). <https://doi.org/10.1146/annurev-biochem-060208-092442>
- [24] Nillegoda, N. B., Wentink, A. S., Bukau, B. Protein disaggregation in multicellular organisms. *Trends Biochem. Sci.* 43, 285-300 (2018). <https://doi.org/10.1016/j.tibs.2018.02.003>
- [25] Wyatt, A. R., Yerbury, J. J., Dabbs, R. A., Wilson, M. R. Roles of extracellular chaperones in amyloidosis. *J. Mol. Biol.* 421, 499-516 (2012). <https://doi.org/10.1016/j.jmb.2012.01.004>
- [26] Tang, H. D., Fu, Y., Zhan, S. L., Luo, Y. Z.  $\alpha_E C$ , the c-terminal extension of fibrinogen, has chaperone-like activity. *Biochemistry* 48, 3967-3976 (2009). <https://doi.org/10.1021/bi900015n>
- [27] Tang, H. D., Fu, Y., Cui, Y. J., He, Y. B., Zeng, X., Ploplis, V. A., et al. Fibrinogen has chaperone-like activity. *Biochem. Biophys. Res. Commun.* 378, 662-667 (2009). <https://doi.org/10.1016/j.bbrc.2008.11.112>
- [28] Smith, S. G., Walter, L. G., Walker, M. R. Chapter 18-clinical pathology in non-clinical toxicology testing. in Haschek and rousseaux's handbook of toxicologic pathology (Haschek, M. W., Rousseaux, G. C., Wallig, A. M. eds.) vol. I, pp. 565-594 (Academic Press, Amsterdam; Boston, 2013).
- [29] Weisel, J. W. Fibrinogen and fibrin. *Adv. Protein Chem.* 70, 247-299 (2005). [e190017\\_9](https://doi.org/10.1016/S0065-</a></p></div><div data-bbox=)

[3233\(05\)70008-5](https://doi.org/10.2196/3233(05)70008-5)

- [30] Glatter, O., Kratky, O. Small angle x-ray scattering (Academic Press, London; New York, 1982).
- [31] Yamamoto, N., Inoue, R., Makino, Y., Shibayama, N., Naito, A., Sugiyama, M., et al. Structural development of amyloid precursors in insulin B chain and the inhibition effect by fibrinogen. bioRxiv (2021). <https://doi.org/10.1101/2021.12.26.474222>
- [32] Vestergaard, B., Groenning, M., Roessle, M., Kastrop, J. S., van de Weert, M., Flink, J. M., et al. A helical structural nucleus is the primary elongating unit of insulin amyloid fibrils. PloS Biol. 5, 1089-1097 (2007). <https://doi.org/10.1371/journal.pbio.0050134>
- [33] Oliveira, C. L. P., Behrens, M. A., Pedersen, J. S., Erlacher, K., Otzen, D., Pedersen, J. S. A SAXS study of glucagon fibrillation. J. Mol. Biol. 387, 147-161 (2009). <https://doi.org/10.1016/j.jmb.2009.01.020>
- [34] Luo, J. H., Warmlander, S. K. T. S., Graslund, A., Abrahams, J. P. Non-chaperone proteins can inhibit aggregation and cytotoxicity of alzheimer amyloid  $\beta$  peptide. J. Biol. Chem. 289, 27766-27775 (2014). <https://doi.org/10.1074/jbc.M114.574947>

---

This article is licensed under the Creative Commons Attribution-NonCommercial-ShareAlike 4.0 International License. To view a copy of this license, visit <https://creativecommons.org/licenses/by-nc-sa/4.0/>.

